Green Chemistry

PAPER

View Article Online
View Journal

Cite this: DOI: 10.1039/c3gc42545b

Co-immobilization of multi-enzyme on control-reduced graphene oxide by non-covalent bonds: an artificial biocatalytic system for the one-pot production of gluconic acid from starch†

Fuhua Zhao,[a,b] Hui Li,[c] Yijun Jiang,*[a] Xicheng Wang[a] and Xindong Mu*[a]

Received 14th December 2013,
Accepted 13th January 2014

DOI: 10.1039/c3gc42545b

www.rsc.org/greenchem

Here we report a simple and efficient approach to fabricate a new biocatalytic system by co-immobilizing multi-enzyme on chemically reduced graphene oxide (CRGO) *via* non-covalent bonds. The obtained artificial biocatalyst was characterized by UV/Vis, FTIR, AFM, TEM and SEM. Compared with native and graphene oxide (GO) bounded enzymes, it was found that the glucose oxidase (GOD) or glucoamylase (GA) immobilized on CRGO exhibited significantly higher enzymatic activity, due to the positive effect of the CRGO carrier. This multi-enzyme microsystem was employed as a biocatalyst to accomplish the starch-to-gluconic acid reaction in one pot, and the yield of gluconic acid could reach 82% within 2 hours. It was also proved that the stability of the multi-enzyme biocatalyst immobilized on CRGO was dramatically enhanced compared with the GO microsystem. About 85% of the activity of the artificial biocatalyst could be preserved after four cycles. These results demonstrated the feasibility of the novel strategy to construct bio-microsystems with multi-enzyme on 2D CRGO *via* non-covalent bonds to accomplish some complex conversions.

1. Introduction

Enzymes are native catalysts. In living cells, a number of enzymes often work together in multi-step reactions or cascade processes. Efficient transfer of the intermediates from one catalytic site to another is achieved by the formation of macromolecular enzyme complexes. This so-called metabolic channeling has inspired researchers to bring biocatalysts together in an artificial way.[1]

Multi-step enzymatic synthesis can be carried out by adding multiple enzymes to the same reaction vessel.[2–4] In order to improve the reusability and stability of the biocatalysts, different enzymes can be linked to the same support by co-immobilization to mimic multi-enzyme complexes present in cellular systems. Multi-enzymes can be covalently bound to an insoluble carrier.[5,6] Multipoint covalent immobilization can lead to rigidification of the enzyme and thus increase enzyme stability. However, in some cases enzymatic activity is negatively affected. As an alternative, non-covalent methods of physical encapsulation were developed to avoid the negative influences on the structure of the enzyme. Kreft and co-workers[7] presented a general method for the preparation of micrometer-sized shell-in-shell polyelectrolyte capsules by deposition of polyelectrolyte multilayers. In their capsule system the enzyme was separated by a semi-permeable membrane. Betancor *et al.*[8] co-immobilized nitrobenzene nitroreductase and glucose-6-phosphate dehydrogenase in silica particles by co-encapsulation, which enabled the continuous conversion of nitrobenzene to hydroxylaminobenzene with nicotinamide adenine dinucleotide phosphate recycling. Zhang *et al.*[9] also reported a multicompartment multi-enzyme system by spontaneous self-polymerization of dopamine on the surface of a $CaCO_3$ microparticle template. Although physical encapsulation is an effective method for retaining the activities of the enzymes, the process of synthesis is relatively complex and the reaction rate is fairly low due to diffusion problems of the substrates. Therefore, it is desirable to develop new strategies for the design and assembly of multi-enzyme systems with simple processing and at the same time achieve a system can also retain or increase the enzyme activities.

Graphene oxide (GO), as a precursor of graphene, has attracted huge attention because of its unique physical and chemical properties, thus been widely applied in various

[a]Key Laboratory of Bio-based Materials, Qingdao Institute of Bioenergy and Bioprocess Technology, Chinese Academy of Sciences, Qingdao, 266101, China. E-mail: jiangyj@qibebt.ac.cn, muxd@qibebt.ac.cn; Fax: +86-532-80662724; Tel: +86-532-80662725
[b]University of Chinese Academy of Sciences, Beijing 100049, PR China
[c]Key Laboratory of Marine Chemistry Theory and Technology, Ministry of Education, Ocean University of China, Qingdao, 266100, China
†Electronic supplementary information (ESI) available. See DOI: 10.1039/c3gc42545b

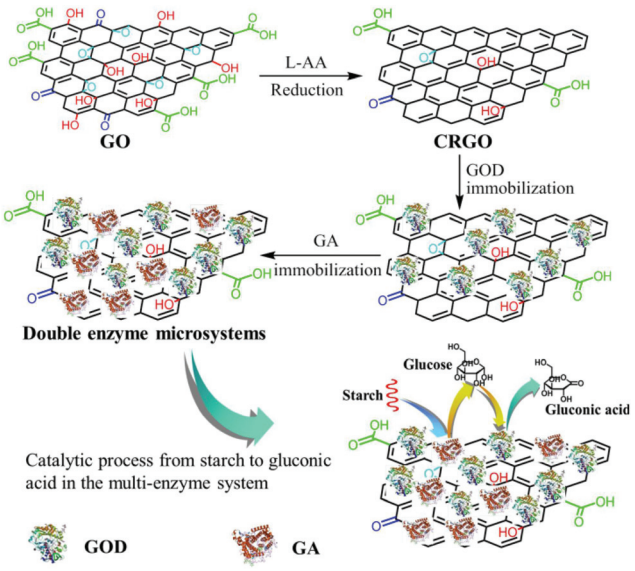

Scheme 1 Schematic representation of the GO reduction, the construction of the multi-enzyme microsystem and the one-pot conversion of starch into gluconic acid.

fields.[10–13] Among them, the incredibly large specific surface area (single-layered and unique double-sided), abundant oxygen-containing groups (such as hydroxyl, epoxy, carbonyl and carboxyl groups), and high water solubility make it an ideal carrier for enzyme immobilization.[14–18] Chemically reduced graphene oxide (CRGO), lack of surface functional groups but kept the single-layered and 2D structure, is a promising candidate for enzyme immobilization to improve the performance of immobilized enzyme.[19]

Inspired by the metabolic channelling of live cells, herein, we constructed an artificial biomimetic microsystem by co-immobilizing GOD and GA onto a 2D carrier (CRGO) to accomplish the direct one-pot conversion of starch to gluconic acid. Although there has been some work on co-immobilizing GA and GOD onto other carriers,[20–23] most of them were fixed on an electrode for use as a biofuel cell or a biosensor. To the best of our knowledge, this is the first report on the immobilization of multi-enzymes (GOD and GA) on a 2D CRGO carrier to construct an artificial microsystem to convert starch into gluconic acid in one pot. Interestingly, it was found the activity and reusability of the enzymes, especially GOD immobilized on CRGO, could be improved dramatically by controlling the extent of GO reduction. The sketch map of GO reduction, multi-enzyme immobilization and the catalytic process from soluble starch to gluconic acid is proposed in Scheme 1. This approach may provide a novel strategy to construct *in vitro* multi-enzymatic assemblies.

2. Experimental

2.1. Materials

GOD (50 000 U g^{-1}) and GA (100 000 U mL^{-1}) from *Aspergillus niger* were purchased from Aladdin. Graphite was obtained from Sigma-Aldrich, Co., Ltd. All other reagents were of analytical grade from Sinopharm Chemical Reagent Co., Ltd and used without further purification.

2.2. Preparation of GO

GO was prepared using natural graphite flakes by a modified Hummers method.[24,25] In a typical procedure, 2.04 g of graphite flakes were mixed with 50 mL of concentrated sulfuric acid in a 100 mL reaction flask and the mixture was cooled in an ice bath with constant stirring. After that, 6.13 g of $KMnO_4$ was added very slowly over 2 h at 0 °C, obtaining a dark mixture. The mixture was then stirred at 0 °C for 1 h and an additional 2 h at room temperature, and subsequently heated to 35 °C for 3 h. After cooling to room temperature, the mixture was slowly poured into 1 L of deionized (DI) water, followed by the addition of 5 mL of 30% H_2O_2, resulting in a bright yellow mixture. The yellow mixture was centrifuged and the isolated materials were washed with 1 L of 6 M HCl solution and large amounts of DI water until a neutral pH was obtained. Finally, the product was dried at 50 °C under vacuum for 24 h to afford a dark brown solid.

2.3. Preparation of CRGO

CRGO was prepared by the reduction of GO sheets with L-ascorbic acid (L-AA) at room temperature.[26] In brief, GO was exfoliated into GO sheets by ultrasonication (37 Hz) in water for 2 h to give a 0.5 mg mL^{-1} colloidal solution. Then 0.5 g of L-AA was directly added into 100 mL of the aforementioned GO dispersion under vigorous stirring. The reduction product was separated by centrifugation at 12 000 rpm for 30 min and washed three times with DI water to remove redundant L-AA.

2.4. Enzyme immobilization

GOD and GA were respectively immobilized on the GO or CRGO to investigate the activities of the enzymes before and after immobilization. Then, the two kinds of enzymes were co-immobilized onto the GO or CRGO carrier to obtain a multi-enzyme system. For the immobilization single enzymes on the GO, the GA, GOD and GO were first dispersed in acetate buffer solution (0.1 M, pH 4), respectively. The desired amount of GO dispersion was added into the GA or GOD enzyme solution to form a mixture, in which the concentrations of the enzyme and GO were both 1 mg mL^{-1}. The mixture was incubated at 4 °C for 4 h with occasional shaking, followed by being centrifuged at 7000 rpm for 10 min. The supernatant was collected to determine the enzyme loading using the Lowry method.[27] The solids were centrifuged and rinsed alternately three times with the same buffer to remove nonspecific adsorbed enzymes. The amount of the immobilized enzyme was evaluated by the enzyme concentration change of the solution before and after loading. For the single enzyme immobilization on CRGO a similar procedure was applied except that a pH 5 buffer and a CRGO dispersion were used. For the co-immobilization, GOD was immobilized onto the carrier first (the concentration of GOD in the mixture was 0.5 mg mL^{-1}), and GA was subsequently immobilized onto the GOD-bound

carrier (the concentration of GA in the mixture was 1 mg mL^{-1}). Other conditions were the same as for the single enzyme immobilization procedure.

2.5. Activity assay

The activity of GOD and GA were measured using glucose or soluble starch as the substrate, respectively, and evaluated by calculating the rate of the gluconic acid (GOD) or glucose production (GA) under the standard conditions. The activity of co-immobilized multi-enzyme microsystem was measured using soluble starch as a substrate and determined by calculating the rate of the gluconic acid production released from the initial substrate. The control experiments without any enzyme were performed, no glucose or gluconic acid was generated when just using CRGO as a catalyst.

2.6. Characterizations

UV/Vis spectra were recorded on a UV-250 spectrophotometer. Fourier-transform infrared (FTIR) spectra of the samples were recorded in the range of 4000 to 600 cm^{-1} using a Nicolet 6700 FTIR spectrometer (ThermoFisher). The specimens were prepared by grinding the dried analyte with KBr and pressing the mixture into tablets. Transmission electron microscopy (TEM) images were recorded on a Hitachi H-7650 transmission electron microscope at 100 kV. Samples were prepared by applying a drop of the GO or CRGO ethanol suspension onto a carbon-coated copper grid and dried at room temperature. Atomic force microscopy (AFM) was performed using the tapping mode on a MultiMode Nanoscope V scanning probe microscopy system (Agilent 5400 AFM). The samples for AFM were prepared by depositing the aqueous dispersion on a freshly cleaved mica surface. Scanning electron microscopy (SEM) images were recorded on Hitachi S-4800 equipment. Prior to imaging, the samples were sputter-coated with gold thereby making the samples conductive.

2.7. HPLC analysis

The analysis of glucose and gluconic acid was performed on a Agilent 1100 high performance liquid chromatography (HPLC) equipped with a variable wavelength detector (VWD) and a refractive index detector (RID).[28] A BioRad Aminex HPX-87H column thermostated at 55 °C was used with H_2SO_4 (0.05 M) as the eluent. A certain amount of NaOH solution was added into the samples as soon as they were taken out of the reaction mixture to ensure that the enzymes in the samples were inactivated and H_2O_2 had decomposed before detection.

3. Results and discussion

3.1. Characterization of the materials

The reduction degree of CRGO was regulated by the reaction time: the longer the reaction time, the greater the reduction degree, which was monitored using UV/Vis and FTIR spectroscopy. As shown in Fig. 1a (inset), GO showed a main plasmon peak at around 232 nm, representing the π–π*

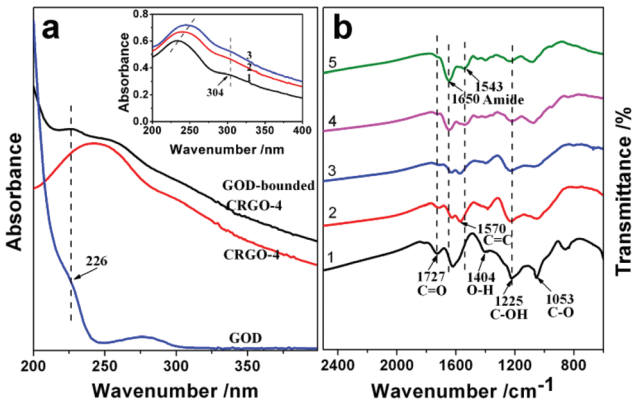

Fig. 1 UV/Vis spectra (a) of GOD, CRGO-4 and GOD-bound CRGO-4. FTIR spectra (b) of the GO (1), CRGO-2 (2) and CRGO-4 (3), GOD-bound CRGO-4 (4) and multi-enzyme immobilized CRGO-4 (5). The inset panel shows the UV/Vis spectral of GO (1), CRGO-2 (2) and CRGO-4 (4).

transition of aromatic C=C, and a shoulder at around 304 nm, attributed to the n–π* transition of C=O.[29,30] Upon reduction with L-AA, the plasmon peak at 232 nm shifted gradually to 239 and 245 nm for CRGO-2 and CRGO-4 (CRGO-2 and CRGO-4 represent GO reduced with L-AA for 2 and 4 h, respectively), respectively; the shoulder peak at around 304 nm decayed gradually with the reduction time. The red-shift of the plasmon peak at 232 nm and the decay of the shoulder peak suggested the reduction of GO and that the aromatic structure might be restored, which was further confirmed by FTIR spectroscopy. As shown in Fig. 1b (1–3), GO gave several strong characteristic peaks corresponding to the oxygen functionalities, such as the C=O stretching vibration peak at 1727 cm^{-1}, O–H deformations in the C–OH groups at 1404 cm^{-1}, C–OH stretching vibration peak at 1225 cm^{-1} and C–O stretching vibrations peak in C–O–C of epoxide at 1053 cm^{-1}.[31,32] However, the peak intensity of the oxygen functional groups decreased with the reduction time, and the skeletal vibration absorption peak of graphene at about 1570 cm^{-1} was observed,[33] indicating the successful restoration of the partial aromatic ring structure. Furthermore, the hydrophobicity of CRGO was enhanced compared with GO. A pictorial presentation is shown in Fig. 2c. The samples in the picture were blended by ultrasonic dispersing and then allowed to stand for 3 minutes. Obviously, the dispersion of GO and enzyme loaded CRGO-2 was still preferable after standing for 3 minutes while CRGO-2 gathered and precipitated rapidly. This was because the abundant oxygen-containing groups (such as hydroxyl, epoxy, carbonyl and carboxyl groups) on the GO surface resulted in a high water solubility; after reduction, the oxygen-containing groups were decreased, which lead to better hydrophobicity and worse water solubility. However, when amphiphilic enzymes were immobilized onto the CRGO, oxygen-containing groups were introduced by the enzymes and the dissolubility was recovered (Fig. 2c).

The successful loading of enzymes was confirmed by UV/Vis and FTIR spectroscopy, represented by CRGO-4. As can be seen in Fig. 1a, the pattern of the UV spectrum of the

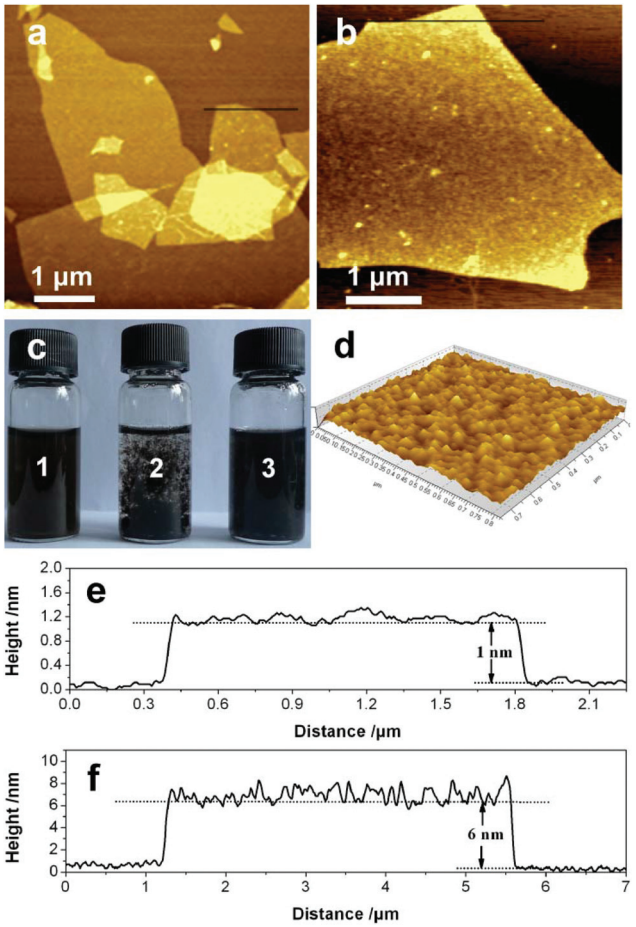

Fig. 2 Tapping mode AFM images of (a) CRGO-4 and (b) multi-enzyme loaded CRGO-4. (c) A pictorial presentation of dispersion liquid in pH 5, 0.1 M of PBS (C1: 0.25 mg mL^{-1} of GO; C2: 0.25 mg mL^{-1} of CRGO-2; C3: 0.25 mg mL^{-1} of enzyme loaded CRGO-2). (d) AFM 3D image of a detail of the GOD and GA on the surface of CRGO-4. The height profile of the AFM images of (e) CRGO and of (f) multi-enzyme loaded CRGO-4.

enzyme-loaded CRGO is significantly different from that of CRGO. The C=C plasmon peak at about 245 nm was retained, but the absorption before 245 nm was dramatically increased and a new absorption peak appeared at about 226 nm, which was in accordance with the peak of GOD, indicating the successful combination of GOD and CRGO. Furthermore, comparison of curves 3 and 4 in Fig. 1b, show that new bands at about 1650 cm^{-1} and 1543 cm^{-1} have emerged, which correspond to the C=O stretching vibrations of amide I band and N–H bending vibrations of amide II band in the infrared spectra of the protein,[34] demonstrating the GOD loading on the CRGO carrier. Moreover, the intensity of the amide peaks in curve 5 are increased compared with curve 4, which might be caused by the additional peak of GA on GOD-bound CRGO. The above observations all proved that the multiple enzymes were successfully immobilized on the 2D CRGO carriers.

The morphology of each of the as-prepared samples was characterized using AFM and TEM. They all proved that CRGO was successfully prepared with a 2D structure. The height profile of the AFM images verified that the thickness of the CRGO sheet was about 1 nm (Fig. 2e), demonstrating that the sheet morphology of the GO was maintained after reduction and a single atomic layer thickness structure was obtained, which was in agreement with the TEM images (Fig. S1a and b†). The enzyme loading on the CRGO was further proved by surface morphology analysis. Typical AFM images of CRGO before and after enzyme loading are shown in Fig. 2a and b. As expected, the CRGO sheet exhibited a fairly smooth surface (Fig. 2a) before enzyme loading, however, it became quite rough after enzyme loading (Fig. 2b), and the 3D image (Fig. 2d) clearly showed that the enzyme molecules densely covered the entire surface of the CRGO sheets. The thickness of the sheets, measured from the height profile of the AFM image, increased from 1 nm to 6 nm (Fig. 2e and f), confirming that the CRGO sheet was fully covered by the enzyme. Alternatively, Hecht *et al.* reported the crystal structure of GOD, whose size was about 6 nm × 5 nm × 7.7 nm,[35] and the diameters of the catalytic domain and binding domain within GA were reported to be 5.9 nm and 3.4 nm, respectively.[36] These results indicated that the multi-enzyme was immobilized on the 2D graphene-based material with a single layer. The shorter height of the immobilized enzyme molecules revealed that the immobilization may induce some conformational changes in the enzyme molecules.[15]

3.2. Optimization of reaction conditions and activity assay

GOD and GA were immobilized at pH 5 on CRGO-2, CRGO-4 and CRGO-12 (CRGO-12 represents GO reduced with L-AA for 12 h), respectively, without the use of a coupling reagent. For the co-immobilized enzymes, the loadings of GOD and GA on GO were 0.331 and 0.132 mg mg^{-1}, respectively, and that on CRGO-2 were 0.299 and 0.205 mg mg^{-1}, respectively. Immobilized enzymes usually exhibit enhanced stability but lower activity compared to the free enzymes. The loss of activity mainly results from the immobilization procedure and the mass-transfer limitations in solid supports.[37–39] Before our experiments, the activities of each free and immobilized GOD and GA were evaluated to determine the optimal reaction conditions.

The catalytic performances of GA before and after immobilization were investigated using soluble starch as a substrate and that of GOD was researched using glucose as a substrate. As shown in Fig. 3, it was found that the optimum reaction temperature and pH for free GA were 55 °C and 5, respectively. After immobilizing GA on CRGO-2, the optimal temperature became higher (60 °C, Fig. 3a). Under higher temperature or pH conditions, the immobilized GA could also retain relatively higher original activity. For free GOD, the optimal reaction conditions were a temperature of 50 °C and a pH of 5.5. For GOD immobilized on CRGO-2, the optimal reaction temperature was still 50 °C, while the optimal pH became 5, lower than that of the free one (Fig. 3a). It is worth noting that under the same conditions, the immobilized GOD could retain its activity better than the free one due to the protection of the carrier (Fig. 3a). At the same time, the optimum pH range

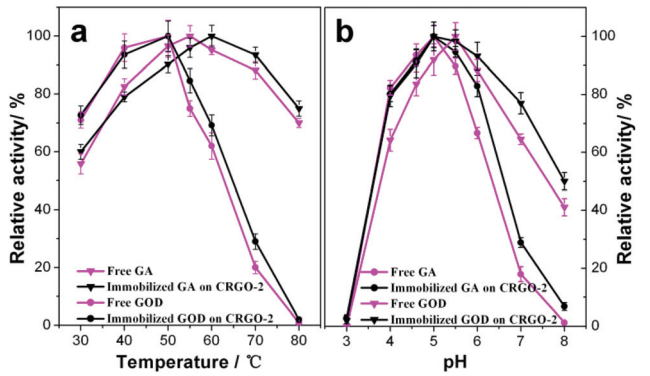

Fig. 3 Effect of temperature (a) and pH (b) on the activity of immobilized GOD on CRGO-2 and immobilized GA on CRGO-2. The highest activity of each enzyme under its optimum temperature or pH was set to 100%.

became broader than the free one. In a word, after immobilization on the 2D CRGO by non-covalent bonding, the GA and GOD possessed a good environmental tolerance (temperature and pH, respectively).

To study the impact of the reduction extent of the CRGO on the activity of the individual enzyme, the enzymatic activities of GA or GOD immobilized on GO, CRGO-2, CRGO-4 and CRGO-12 sheets were quantified for evaluation through their comparison with native GA or GOD under their optimal reaction conditions. As shown in Fig. 4a, compared with free GA, the activities of GA loaded on CRGO-2 and CRGO-4 had an increase of 13.4% and 6%, while that of GA loaded on GO and CRGO-12 had a decrease of 2% and 12%, respectively. Fig. 4b showed that the enzymatic activities of GOD immobilized on GO, CRGO-2 and CRGO-4 exhibited a 27.3%, 111% and 44.4% increase, respectively, compared with the activity of free GOD in solution, while that of GOD immobilized on CRGO-12 had a little drop (10%). Similarly, it was found that the catalytic activity of the immobilized multi-enzyme on the CRGO-2 was also improved compared to its free form in solution (Fig. S6†). It is worth noting that the amount of enzyme loaded on the

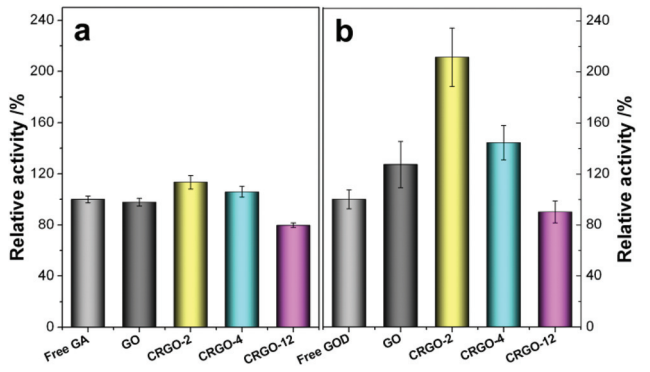

Fig. 4 Relative specific activity of the native GA and the GA bound to GO or CRGO (a), and of the native GOD and the GOD bound to GO or CRGO (b). The specific activity of free enzyme was set to 100%.

CRGOs was closely associated with its reduction extent: the greater the reduction degree, the higher the enzyme loading. The maximum loadings of GA on CRGO-2, CRGO-4 and CRGO-12 were 0.64, 0.83, and 1.6 mg mg^{-1}, respectively, and that of GOD were 0.25, 0.34, and 0.55 mg mg^{-1}, respectively. Based on the FTIR results, the hydrophilic functional groups (OH, COOH) on the support were diminished during the reduction, indicating that the hydrophobicity of CRGO was enhanced, which can also be proved by the fact that the dispersibility of GO in water declined with reduction time (Fig. 2c). Consequently, we concluded that the binding of the enzymes to CRGO was mainly through hydrophobic interactions, and the increasing hydrophobic interaction between enzyme and CRGO lead to the higher enzyme loading when the support was reduced for a longer time, which is consistent with the earlier report.[19] It is interesting that the GA or GOD immobilized CRGO-2 matrix showed the highest activity, and that the longest time of GO reduction resulted in the lowest activity (Fig. 4), which strongly indicated that it was important to control the surface hydrophobicity of GO to improve the activities of the enzymes in our experiments. Based on the structure analysis of AFM and FTIR, a conformational change may occur in the enzymes immobilized on the CRGO because of the hydrophobic combination between the carrier and enzymes. The slight conformational change might lead to an increased activity for the enzyme immobilized on the CRGO which was reduced for a shorter time. However, with the increase of reduction time, stronger hydrophobic interactions between CRGO and the enzyme occur and cause the conformation of the enzyme to seriously deform, which may lead to inactivation of the immobilized enzyme. In other words, appropriate interactions between the carrier and enzyme can increase its activity, or else the activity will be decreased, that is why we chose CRGO-2 as the carrier to immobilize enzymes in this paper. These results also agree well with previous reports.[19] Additionally, in our method, the enzymes were immobilized on the 2D surface of the GO-based carrier, which did not result in a mass-transfer limitation like for other methods and carriers (such as encapsulation with other polymers or inorganic carriers), thus making it possible to retain a relatively high activity of the enzyme loaded on its surface.

Based on the study of the single enzyme, we tried to co-immobilize the two kinds of enzymes on the CRGO-2 carrier to obtain a multi-enzyme microsystem, which was used to catalyze the conversion of starch to gluconic acid in one pot, just like a living cell. In our experiments, we tried two methods to introduce the two kinds of enzymes onto the surface of the GO-based carriers. One way was to fix GA and GOD simultaneously using the mixture solution of the two kinds of enzymes. However, it was found that it was difficult to control the amount of each enzyme fixed on the carrier due to their different hydrophobic properties. The other way was to immobilize one enzyme first and then the other. This method had the advantage of being able to control the loading amounts of the enzymes. So, in our experiments, we used the second method to fabricate the multi-enzyme system.

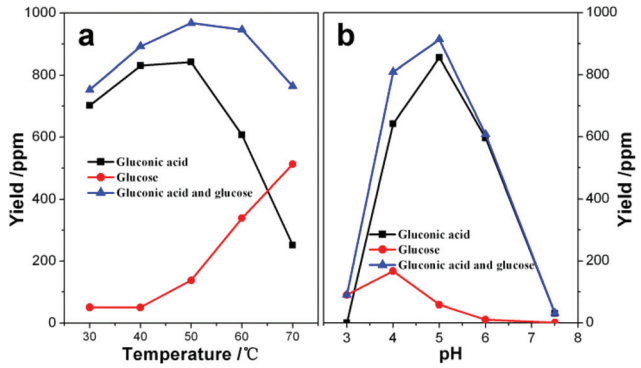

Fig. 5 Effect of temperature (a) and pH (b) of the multi-enzyme microsystem. Concentration of the multi-enzyme biocatalyst is 0.2 mg mL^{-1} and of initial soluble starch is 1 mg mL^{-1}.

Based on the above single enzyme reaction conditions, we optimized them for the multi-enzyme microsystem. Fig. 5 shows that the largest yield of gluconic acid was achieved at a temperature of 50 °C and pH of 5, which was similar to the single enzyme. Therefore, all the reactions catalyzed by the multi-enzyme system in this work were under these conditions.

The process of the multi-enzyme system for simultaneous hydrolysis and oxidation in one pot to convert starch to gluconic acid was investigated (Fig. 6). It was found that the concentration of glucose increased within 45 minutes and then decreased, meanwhile the yield of gluconic acid had a linear increase during the whole reaction process. It is believed that the starch was first hydrolyzed into glucose, and then glucose was further converted into gluconic acid, catalyzed by the GOD in the multi-enzyme biocatalyst. However, the rate of hydrolysis of starch was much faster than that of the oxidation of glucose (Fig. S3†), so glucose was accumulated in the first 45 min. After that, the reaction of starch hydrolysis was close to the end, and the consumption of glucose was more than the production, therefore the content of glucose began to reduce and gluconic acid increased. Three hours later, the starch-to-gluconic acid conversion reached 72%. It should be noted that the reaction rate involved with these two enzymes could be controlled by regulating the amounts and proportions of the enzymes. When regulating the mass ratio of GA : GOD loaded on the CRGO-2 carrier to 1 : 1.3, the conversion of starch to gluconic acid reached 82% (Fig. S4†) within 2 hours. Importantly, this process has a high selectivity for gluconic acid (more than 99% detected *via* HPLC), just like the other biocatalyst system.

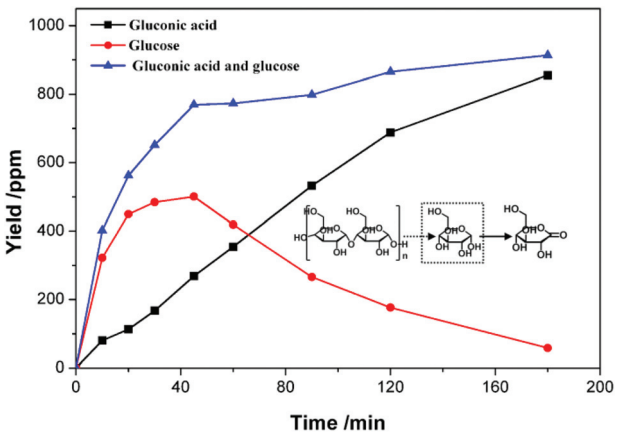

Fig. 6 The enzymatic process of the microsystem for starch hydrolysis coupled with glucose oxidation in one pot at 50 °C and pH 5. Concentration of the multi-enzyme biocatalyst is 0.2 mg mL^{-1} and of initial soluble starch is 1 mg mL^{-1}. The mass ratio of GA : GOD loaded on the CRGO-2 carrier is 1 : 0.8.

3.3. Reusability

The reusability of immobilized enzymes is always a concern. In our system, the recycling ability of the multi-enzyme microsystems, immobilized on the 2D GO-based material by non-covalent bonds, was also investigated. The specific activity of the first run was set to 100%. The yield of the final target product (gluconic acid) was used to evaluate the catalytic activities of the artificial microsystems. As shown in Fig. 7, the artificial multi-enzyme immobilized on CRGO-2 could retain about 85% of its original activity after four cycles; while the GO immobilized system can just only retain 10% of the initial activity under the same conditions. The obvious difference between GO and CRGO-2 in the reusability test could probably be ascribed to the different interactions between the enzymes and carriers. As aforementioned, the interactions between the enzyme molecules and the GO surface are electrostatic interactions, which are very sensitive to the environment (such as pH, ionic strength, *etc.*). In our system, the pH value of the catalytic reaction was higher than that of the immobilization and the isoelectric point (PI) of the GA and GOD, so the balance of the interactions between the enzymes and GO was broken and the enzymes were detached from the substrate during the reaction, which led to the poor reusability. However, the driving force between the enzymes and CRGO was mainly hydrophobic interactions, which was barely affected by pH changes. Therefore, the reusability was dramatically improved. This result is

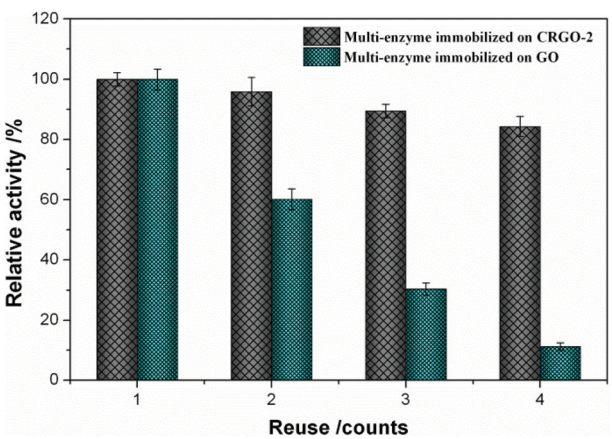

Fig. 7 Reuse of the double enzyme microsystem on GO and CRGO-2. The enzymatic activity of the first round was set to 100%.

consistent with the structure analysis of the GO and CRGO surfaces. In addition, the thermal stability of free and immobilized multi-enzyme system was also investigated at 50 °C (Fig. S5†). It was found that the thermal stability of the immobilized multi-enzyme system was obviously enhanced compared with the free forms. This may be another reason why the reusability was improved compared to the GO system. However, deactivation still occurred over time and lower enzyme leakage still can be detected in our CRGO system, which may be the reasons why the activity still has a little drop during the recycling.

4. Conclusions

In summary, we successfully employed a non-covalent method to co-immobilize multi-enzymes (GOD and GA) onto a 2D GO-based material to fabricate an artificial bio-microsystem, which could act as an efficient biocatalyst in the one-pot conversion of starch to gluconic acid. The artificial bio-microsystem exhibited a relatively high starch-to-gluconic acid conversion efficiency and selectivity (82% yield and 99% selectivity), as well as a commendable reusability. Compared with the GO-enzyme conjugate, the CRGO-enzyme conjugates exhibited better stability and higher activity. Importantly, this approach provides a novel strategy to construct the *in vitro* multi-enzymatic assembling in the bio-field.

Acknowledgements

This work was supported by the Natural Science Foundation of China and Shandong Province (no. 21003146, ZR2010BQ014), Shandong Province Foundations for Outstanding Young Scientists (JQ201305) and Chinese Academy of Sciences (no. KSCX2-EW-J-10).

Notes and references

1 S. Schoffelen and J. C. van Hest, *Soft Matter*, 2012, **8**, 1736–1746.
2 C. J. Thibodeaux, C. E. Melançon and H. W. Liu, *Nature*, 2007, **446**, 1008–1016.
3 Z. Findrik and Đ. Vasić-Rački, *Chem. Biochem. Eng. Q.*, 2009, **23**, 545–553.
4 K. M. Koeller and C. H. Wong, *Chem. Rev.*, 2000, **100**, 4465–4494.
5 K. Mosbach and B. Mattiasson, *Acta Chem. Scand.*, 1970, **24**, 2093–2100.
6 U. Hanefeld, L. Gardossi and E. Magner, *Chem. Soc. Rev.*, 2009, **38**, 453–468.
7 O. Kreft, M. Prevot, H. Möhwald and G. B. Sukhorukov, *Angew. Chem., Int. Ed.*, 2007, **46**, 5605–5608.
8 L. Betancor, C. Berne, H. R. Luckarift and J. C. Spain, *Chem. Commun.*, 2006, 3640–3642.
9 L. Zhang, J. Shi, Z. Jiang, Y. Jiang, S. Qiao, J. Li, R. Wang, R. Meng, Y. Zhu and Y. Zheng, *Green Chem.*, 2011, **13**, 300–306.
10 Z. Liu, J. T. Robinson, X. Sun and H. Dai, *J. Am. Chem. Soc.*, 2008, **130**, 10876–10877.
11 J. R. Lomeda, C. D. Doyle, D. V. Kosynkin, W. F. Hwang and J. M. Tour, *J. Am. Chem. Soc.*, 2008, **130**, 16201–16206.
12 Y. Xu, Z. Liu, X. Zhang, Y. Wang, J. Tian, Y. Huang, Y. Ma, X. Zhang and Y. Chen, *Adv. Mater.*, 2009, **21**, 1275–1279.
13 D. Li, M. B. Müller, S. Gilje, R. B. Kaner and G. G. Wallace, *Nat. Nanotechnol.*, 2008, **3**, 101–105.
14 S. Alwarappan, C. Liu, A. Kumar and C. Z. Li, *J. Phys. Chem. C*, 2010, **114**, 12920–12924.
15 J. L. Zhang, F. Zhang, H. J. Yang, X. L. Huang, H. Liu, J. Y. Zhang and S. W. Guo, *Langmuir*, 2010, **26**, 6083–6085.
16 F. Zhang, B. Zheng, J. Zhang, X. Huang, H. Liu, S. Guo and J. Zhang, *J. Phys. Chem. C*, 2010, **114**, 8469–8473.
17 Q. Zeng, J. Cheng, L. Tang, X. Liu, Y. Liu, J. Li and J. Jiang, *Adv. Funct. Mater.*, 2010, **20**, 3366–3372.
18 C. Shan, H. Yang, J. Song, D. Han, A. Ivaska and L. Niu, *Anal. Chem.*, 2009, **81**, 2378–2382.
19 Y. Zhang, J. Zhang, X. Huang, X. Zhou, H. Wu and S. Guo, *Small*, 2012, **8**, 154–159.
20 Q. Lang, L. Yin, J. Shi, L. Li, L. Xia and A. Liu, *Biosens. Bioelectron.*, 2014, **51**, 158–163.
21 K. Yamamoto, T. Matsumoto, S. Shimada, T. Tanaka and A. Kondo, *New Biotechnol.*, 2013, **30**, 531–535.
22 K. Bahartan, L. Amir, A. Israel, R. G. Lichtenstein and L. Alfonta, *ChemSusChem*, 2012, **5**, 1820–1825.
23 M. Onda, Y. Lvov, K. Ariga and T. Kunitake, *J. Ferment. Bioeng.*, 1996, **82**, 502–506.
24 W. S. Hummers Jr. and R. E. Offeman, *J. Am. Chem. Soc.*, 1958, **80**, 1339–1339.
25 D. R. Dreyer, H. P. Jia and C. W. Bielawski, *Angew. Chem.*, 2010, **122**, 6965–6968.
26 J. Zhang, H. Yang, G. Shen, P. Cheng, J. Zhang and S. Guo, *Chem. Commun.*, 2010, **46**, 1112–1114.
27 O. H. Lowry, N. J. Rosebrough, A. L. Farr and R. J. Randall, *J. Biol. Chem.*, 1951, **193**, 265–275.
28 S. Biella, L. Prati and M. Rossi, *J. Catal.*, 2002, **206**, 242–247.
29 T. T. Baby and S. Ramaprabhu, *J. Mater. Chem.*, 2011, **21**, 9702–9709.
30 Z. Luo, Y. Lu, L. A. Somers and A. C. Johnson, *J. Am. Chem. Soc.*, 2009, **131**, 898–899.
31 N. Wu, X. She, D. Yang, X. Wu, F. Su and Y. Chen, *J. Mater. Chem.*, 2012, **22**, 17254–17261.
32 H. K. Jeong, H. J. Noh, J. Y. Kim, M. Jin, C. Park and Y. Lee, *Europhys. Lett.*, 2008, **82**, 67004.
33 F. Gong, X. Xu, G. Zhou and Z. S. Wang, *Phys. Chem. Chem. Phys.*, 2013, **15**, 546–552.
34 F. Bonnier, S. Rubin, L. Debelle, L. Venteo, M. Pluot, B. Baehrel, M. Manfait and G. D. Sockalingum, *J. Biophotonics*, 2008, **1**, 204–214.
35 H. Hecht, H. Kalisz, J. Hendle, R. Schmid and D. Schomburg, *J. Mol. Biol.*, 1993, **229**, 153–172.

36 G. F. H. Kramer, A. P. Gunning, V. J. Morris, N. J. Belshaw and G. Williamson, *J. Chem. Soc., Faraday Trans.*, 1993, **89**, 2595–2602.
37 J. Kim, J. W. Grate and P. Wang, *Trends Biotechnol.*, 2008, **26**, 639–646.
38 H. R. Luckarift, J. C. Spain, R. R. Naik and M. O. Stone, *Nat. Biotechnol.*, 2004, **22**, 211–213.
39 C. Mateo, V. Grazu, J. M. Palomo, F. Lopez-Gallego, R. Fernandez-Lafuente and J. M. Guisan, *Nat. Protoc.*, 2007, **2**, 1022–1033.